

**NUMERICAL SIMULATIONS OF FILM  
BOILING AND CONDENSATION OVER  
CIRCULAR CYLINDERS USING INTERFACE  
CAPTURING METHODS**

**S M THAMIL KUMARAN**



**DEPARTMENT OF MECHANICAL ENGINEERING**

**INDIAN INSTITUTE OF TECHNOLOGY DELHI**

**MAY 2024**

© Indian Institute of Technology Delhi (IITD), New Delhi, 2024

NUMERICAL SIMULATIONS OF FILM BOILING  
AND CONDENSATION OVER CIRCULAR  
CYLINDERS USING INTERFACE CAPTURING  
METHODS

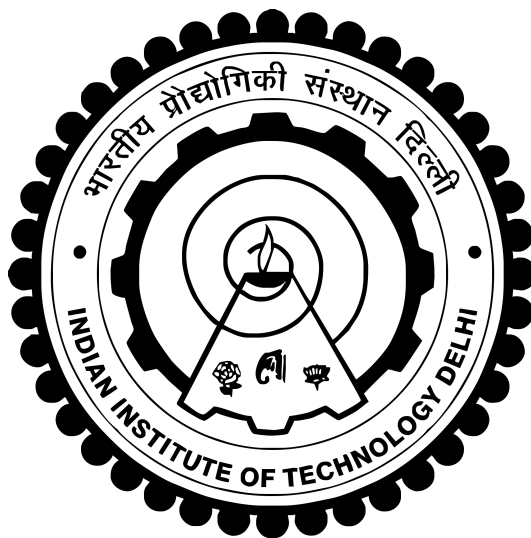
by

**S M Tamil Kumaran**

Department of Mechanical Engineering

Submitted

in fulfilment of the requirements of the degree of Doctor of Philosophy to the



INDIAN INSTITUTE OF TECHNOLOGY DELHI

MAY 2024

**Dedicated to My Father**

# CERTIFICATE

This is to certify that the thesis titled **NUMERICAL SIMULATIONS OF FILM BOILING AND CONDENSATION OVER CIRCULAR CYLINDERS USING INTERFACE CAPTURING METHODS**, submitted by **S M Thamil Kumaran**, to the Indian Institute of Technology, Delhi, for the award of the degree of **Doctor of Philosophy**, is a bona fide record of the research work done by him under our supervision. The contents of this thesis, in full or in parts, have not been submitted to any other Institute or University for the award of any degree or diploma.

**Prof. B Premachandran**  
Professor  
Department of Mechanical Engineering  
Indian Institute of Technology Delhi  
Hauz Khas, New Delhi - 110016  
India

## ACKNOWLEDGEMENTS

The journey towards this dissertation has been a test of my perseverance. However, this journey would not have been wonderful and cherishing without the support and guidance of people to whom I am indebted forever.

I would like to express my gratitude to my supervisor Prof. B Premachadran for his constant guidance and support throughout my PhD. His constant motivation has made me reach this far in my research career. I am indebted for his confidence in me inspite of very long unproductive times in my PhD journey.

I am grateful to my research committee members, Prof. Anjan Ray and Prof. Subhra Datta from the Department of Mechanical Engineering and Prof. Arghya Samanta from the Department of Applied mechanics, for sharing their valuable insights and advice througout my PhD. I also take this opportunity to extend my gratitude towards all my teachers under whom I studied at IIT Delhi and during earlier phases of my education. I also would like to acknowledge the support of Mr. Rajendra Singh and other staff of Department of Mechanical Enigneering for their support.

I would like to thank my friends and fellow research scholars for their immense support throughout my PhD. I take this opportunity to express my gratitude to Mr. Rohit Kumar who had been my constant support at all times of my PhD. I sincerely acknowledge the kindness and warmth I got from my friends and labmates, Dr. Sourab Kumar, Dr. Vijayalakshmi Yerramalle, Dr. B M Ningegowda, Dr. Nikhil Kumar Singh, Dr. Dignpal Kumar, Dr. Sharad Pachpute, Dr. Shital Garg, Mr. Rajesh Kumar, Mr. Nikhil Kattiyar, Mr. B Abhishek, Dr. Vikrant Uday Dupade, Mr. Rubal Prakash, Mr. Shivam and Mr. Manmeet Singh.

I express my gratitude to my parents and my wife for their selfless sacrifices and struggles for my sake. I thank all my relatives for their well wishes and blessings throughout my life.

I humbly bow down at the feet of my Guru with no words to express my gratitude!

**S M Tamil Kumaran**

# ABSTRACT

Phase change phenomena are used to efficiently transport energy in various thermal systems. This is due to the high value of latent heat associated with phase change processes. The phase change phenomena of boiling and condensation are encountered at a wide range of scales in industries from electronic chip cooling to cold storage refrigeration. High heat transfer rates are achieved in the processes involving nucleate boiling and drop-wise condensation. Owing to lower heat transfer rates, the film boiling and film condensation regimes are generally avoided in industrial applications. However, estimates of heat transfer in the film boiling and condensation regimes serve as the limiting cases in boiling and condensation processes. The spatial and temporal scales of the phase change phenomena of film boiling and condensation are small, making the experimental measurements difficult. The theoretical studies on film boiling and condensation involve several simplifying postulations on the interfacial, hydrodynamic and heat characteristics of the phenomena. Direct numerical simulations of two-phase flows with phase change would enable us to improve our understanding of the film boiling and condensation phenomena and will also eliminate the difficulties in the experimental and theoretical analysis of the phenomena.

Interface capturing techniques are one of the important direct numerical simulation methods to simulate multi-phase flows. These techniques capture interfaces on a fixed Eulerian grid, making them computationally cost-effective. Coupled level set and volume of fluid (CLSVOF) is one of the popular and widely used interface capturing techniques. In the present study, a numerical framework using the CLSVOF method is developed to simulate the film boiling phenomenon over circular cylinders. Hence, the two-phase flow solver is developed for two-dimensional unstructured grids, which enable simulations involving curved geometries such as cylinders. The advection of the volume of fluid data is achieved using a

multi-direction geometric algorithm and the advection of the level set field is done using a total variational diminishing (TVD) scheme. Post advection, the level set field is reinitialised using a geometric procedure based on the interface obtained from the volume of fluid (VOF) method. The developed numerical framework is validated with regard to the advection of the level set and volume of fluid data, reconstruction of the interface, surface tension force calculation and phase change calculation on both structured and unstructured grids.

The developed CLSVOF based two-phase flow solver was used to study film boiling over a system of two inline cylinders. The effect of liquid Reynolds number, non-dimensional wall superheat and non-dimensional spacing between the cylinders on the interface dynamics, fluid flow characteristics and heat transfer characteristics were studied. Studies were performed for upward and horizontal liquid flow configurations in the mixed convection regime.

The moment of fluid (MOF) technique is another interface capturing method that has been gaining popularity in recent times. The MOF method can resolve fine interface structures. Hence, it is one of the important direct numerical simulation techniques used for multi-phase flows. In the present work, a numerical framework based on the MOF technique was also developed to simulate film boiling and condensation on two-dimensional unstructured grids. The MOF technique involves the advection of the centroid and volume fraction of one of the phases. The reconstruction of the interface in the MOF technique does not rely on the data from the neighbouring cells and requires only the centroid and volume fraction data of the corresponding cell. In the present work, a face flux based multi-directional advection of material centroid and volume fraction is proposed to enable MOF based two-phase flow simulations on two-dimensional unstructured grids. The developed MOF based two-phase flow solver is validated for its interface reconstruction, material moment advection and surface tension calculation. Using the developed MOF based two-phase flows solver, film condensation over a cylinder is studied. The effect of vapour Reynolds number and the degree of subcooling on the fluid flow and heat transfer characteristics is investigated for the case of downward flow of vapour.

## सार

चरण परिवर्तन घटना का उपयोग विभिन्न थर्मल प्रणालियों में ऊर्जा को कुशलतापूर्वक परिवहन करने के लिए किया जाता है। यह चरण परिवर्तन प्रक्रियाओं से जुड़ी गुप्त ऊष्मा के उच्च मूल्य के कारण है। इलेक्ट्रॉनिक चिप कूलिंग से लेकर कोल्ड स्टोरेज रेफ्रिजरेशन तक उद्योगों में उबलने और संघनन की चरण परिवर्तन घटनाएं व्यापक पैमाने पर सामने आती हैं। न्यूक्लियेट उबलने और बूंद-वार संघनन से जुड़ी प्रक्रियाओं में उच्च गर्मी हस्तांतरण दर प्राप्त की जाती है। कम गर्मी हस्तांतरण दर के कारण, औद्योगिक अनुप्रयोगों में आमतौर पर फिल्म उबलने और फिल्म संक्षेपण व्यवस्था से बचा जाता है। हालाँकि, फिल्म उबलने और संक्षेपण शासन में गर्मी हस्तांतरण का अनुमान उबलने और संघनन प्रक्रियाओं में सीमित मामलों के रूप में काम करता है। फिल्म उबलने और संघनन की चरण परिवर्तन घटना के स्थानिक और लौकिक पैमाने छोटे हैं, जिससे प्रयोगात्मक माप मुश्किल हो जाते हैं। फिल्म उबलने और संघनन पर सैद्धांतिक अध्ययन में घटना की इंटरफेशियल, हाइड्रोडायनामिक और गर्मी विशेषताओं पर कई सरलीकृत धारणाएं शामिल हैं। चरण परिवर्तन के साथ दो-चरण प्रवाह के प्रत्यक्ष संख्यात्मक सिमुलेशन से हमें फिल्म उबलने और संक्षेपण घटना की हमारी समझ में सुधार करने में मदद मिलेगी और घटना के प्रयोगात्मक और सैद्धांतिक विश्लेषण में कठिनाइयों को भी खत्म किया जा सकेगा।

इंटरफ़ेस कैप्चरिंग तकनीक बहु-चरण प्रवाह को अनुकरण करने के लिए महत्वपूर्ण प्रत्यक्ष संख्यात्मक सिमुलेशन विधियों में से एक है। ये तकनीकें एक निश्चित यूलेरियन ग्रिड पर इंटरफ़ेस कैप्चर करती हैं, जिससे वे कम्प्यूटेशनल रूप से लागत प्रभावी बन जाती हैं। सीएलएसवीओएफ (CLSVOF) लोकप्रिय और व्यापक रूप से उपयोग की जाने वाली इंटरफ़ेस कैप्चरिंग तकनीकों में से एक है। वर्तमान अध्ययन में, गोलाकार सिलेंडरों पर फिल्म उबलने की घटना का अनुकरण करने के लिए सीएलएसवीओएफ पद्धति का उपयोग करके एक संख्यात्मक ढांचा विकसित किया गया है। इसलिए, दो-चरण प्रवाह सॉल्वर को दो-आयामी असंरचित ग्रिड के लिए विकसित किया गया है, जो सिलेंडर जैसे घुमावदार ज्यामिति से जुड़े सिमुलेशन को सक्षम बनाता है। द्रव डेटा की मात्रा का संवहन एक बहु-दिशा ज्यामितीय एल्गोरिथ्म का उपयोग करके प्राप्त किया जाता है और स्तर सेट फ्रील्ड का संवहन कुल परिवर्तनीय हासमान (टीवीडी) योजना का उपयोग करके किया जाता है। संवहन के बाद, स्तर सेट फ्रील्ड को द्रव की मात्रा (वीओएफ) विधि से प्राप्त पूर्णांक के आधार पर एक ज्यामितीय प्रक्रिया का उपयोग करके पुनः प्रारंभ किया जाता है। विकसित संख्यात्मक ढांचे को स्तर सेट और द्रव डेटा की मात्रा के संवहन, इंटरफ़ेस के पुनर्निर्माण, सतह तनाव बल गणना और संरचित और असंरचित दोनों ग्रिडों पर चरण परिवर्तन गणना के संबंध में मान्य किया गया है।

विकसित सीएलएसवीओएफ आधारित दो-चरण प्रवाह सॉल्वर का उपयोग दो इनलाइन सिलेंडरों की प्रणाली पर फिल्म उबलने का अध्ययन करने के लिए किया गया था। इंटरफ़ेस गतिशीलता, द्रव प्रवाह विशेषताओं और गर्मी हस्तांतरण विशेषताओं पर तरल रेनॉल्ड्स संख्या, गैर-आयामी दीवार सुपरहीट और सिलेंडरों के बीच गैर-आयामी रिक्ति के प्रभाव का अध्ययन किया गया। मिश्रित संवहन व्यवस्था में उर्ध्व और क्षैतिज तरल प्रवाह विन्यास के लिए अध्ययन किए गए।

द्रव क्षण (एमओएफ) तकनीक एक अन्य इंटरफ़ेस कैप्चरिंग विधि है जो हाल के दिनों में लोकप्रियता हासिल कर रही है। MOF विधि बढ़िया इंटरफ़ेस संरचनाओं को हल कर सकती है। इसलिए, यह बहु-चरण प्रवाह के लिए उपयोग की जाने वाली महत्वपूर्ण प्रत्यक्ष संख्यात्मक सिमुलेशन तकनीकों में से एक है। वर्तमान कार्य में, द्वि-आयामी असंरचित ग्रिड पर फिल्म उबलने और संक्षेपण का अनुकरण करने के लिए एमओएफ तकनीक पर आधारित एक संख्यात्मक ढांचा भी विकसित किया गया था। एमओएफ तकनीक में किसी एक चरण के केन्द्रक और आयतन अंश का संवहन शामिल होता है। एमओएफ तकनीक में इंटरफ़ेस का पुनर्निर्माण पड़ोसी कोशिकाओं के डेटा पर निर्भर नहीं करता है और इसके लिए केवल संबंधित सेल के सेंट्रोइड और वॉल्यूम अंश डेटा की आवश्यकता होती है। वर्तमान कार्य में, दो-आयामी असंरचित ग्रिड पर एमओएफ आधारित दो-चरण प्रवाह सिमुलेशन को सक्षम करने के लिए सामग्री सेंट्रोइड और वॉल्यूम अंश का एक फेस फ्लक्स आधारित बहु-दिशात्मक संवहन प्रस्तावित है। विकसित एमओएफ आधारित दो-चरण प्रवाह सॉल्वर को इसके इंटरफ़ेस पुनर्निर्माण, सामग्री क्षण संवहन और सतह तनाव गणना के लिए मान्य किया गया है। विकसित एमओएफ आधारित दो-चरण प्रवाह सॉल्वर का उपयोग करके, एक सिलेंडर पर फिल्म संक्षेपण का अध्ययन किया जाता है। वाष्प के नीचे की ओर प्रवाह के मामले में वाष्प रेनॉल्ड्स संख्या के प्रभाव और द्रव प्रवाह और गर्मी हस्तांतरण विशेषताओं पर उपशीतलन की डिग्री की जांच की जाती है।

# TABLE OF CONTENT

<b>CERTIFICATE</b>	<b>i</b>
<b>ACKNOWLEDGEMENTS</b>	<b>ii</b>
<b>ABSTRACT</b>	<b>iv</b>
<b>TABLE OF CONTENT</b>	<b>viii</b>
<b>LIST OF FIGURES</b>	<b>xvii</b>
<b>LIST OF TABLES</b>	<b>xix</b>
<b>NOMENCLATURE</b>	<b>xx</b>
<b>1 Introduction</b>	<b>1</b>
1.1 Background . . . . .	1
1.2 Modeling of two-phase flows using direct numerical simulation techniques .	4
1.2.1 Volume of Fluid method . . . . .	6
1.2.2 Level set method . . . . .	6
1.2.3 Coupled level set and volume of fluid (CLSVOF) method . . . . .	7
1.2.4 Moment of Fluid (MOF) method . . . . .	8
1.3 Motivation . . . . .	8
1.4 Organisation of the thesis . . . . .	9
<b>2 Literature Review</b>	<b>11</b>
2.1 Introduction . . . . .	11
2.2 Direct numerical simulations . . . . .	11
2.3 Studies on film boiling . . . . .	18
2.4 Studies on film condensation . . . . .	22
2.5 Summary of the literature review . . . . .	24

2.6	Objectives of the present work . . . . .	25
<b>3</b>	<b>A CLSVOF method for Direct Numerical Simulations of Film Boiling on Unstructured Grids</b>	<b>26</b>
3.1	Introduction . . . . .	26
3.2	Mathematical formulation and numerical methodology . . . . .	27
3.2.1	Governing equations . . . . .	27
3.2.2	CLSVOF method . . . . .	29
3.2.3	Property, surface tension force and heat flux calculation . . . . .	30
3.2.4	Solver details . . . . .	31
3.3	Validation studies . . . . .	35
3.3.1	Advection tests . . . . .	35
3.3.2	Two-phase flow without mass transfer . . . . .	42
3.4	Film boiling studies . . . . .	45
3.4.1	Film boiling over a flat plate . . . . .	46
3.4.2	Film boiling over a cylinder . . . . .	48
3.5	Summary . . . . .	52
<b>4</b>	<b>Mixed Convection Film Boiling over Two Inline Cylinders in Upward Cross-flow</b>	<b>54</b>
4.1	Introduction . . . . .	54
4.2	Problem formulation . . . . .	55
4.2.1	Computational domain and boundary conditions . . . . .	55
4.2.2	Fluid properties and simulation parameters . . . . .	56
4.2.3	Grid independence study . . . . .	58
4.2.4	Validation of the numerical model . . . . .	60
4.3	Results and discussion . . . . .	63
4.3.1	Effect of liquid cross flow Reynolds number . . . . .	63
4.3.2	Effect of degree of wall superheat . . . . .	70
4.3.3	Effect of spacing between cylinders . . . . .	80
4.4	Summary . . . . .	87
<b>5</b>	<b>Mixed Convection Film Boiling over Two Inline Cylinders in Horizontal Cross-flow</b>	<b>90</b>

5.1	Introduction . . . . .	90
5.2	Problem formulation . . . . .	91
5.2.1	Computational domain and boundary conditions . . . . .	91
5.2.2	Fluid properties and simulation parameters . . . . .	93
5.2.3	Grid independence study . . . . .	94
5.2.4	Validation of the numerical model . . . . .	96
5.3	Results and discussion . . . . .	97
5.3.1	Vortex shedding modes . . . . .	98
5.3.2	Effect of Reynolds number . . . . .	102
5.3.3	Effect of wall superheat . . . . .	111
5.3.4	Effect of spacing between the cylinders . . . . .	119
5.4	Summary . . . . .	128
<b>6</b>	<b>A MOF method for Direct Numerical Simulations of Film Boiling and Condensation on Unstructured Grids</b>	<b>131</b>
6.1	Introduction . . . . .	131
6.2	Governing Equations . . . . .	133
6.3	Numerical methodology . . . . .	134
6.3.1	Interface reconstruction . . . . .	136
6.3.2	Proposed face-flux based multi-direction advection of the fluid moments . . . . .	137
6.3.3	Fluid property, Surface tension force and heat flux calculations . . .	142
6.3.4	Solution procedure . . . . .	143
6.4	Validation studies . . . . .	144
6.4.1	Advection test cases . . . . .	144
6.4.2	Two-phase flow without mass transfer . . . . .	149
6.5	Film boiling study . . . . .	155
6.5.1	Free convection film boiling over a flat surface . . . . .	155
6.6	Summary . . . . .	158
<b>7</b>	<b>Film Condensation of Downward Flowing Vapour over a Cylinder</b>	<b>159</b>
7.1	Introduction . . . . .	159
7.2	Problem formulation . . . . .	159

7.2.1	Computational domain and boundary conditions . . . . .	159
7.2.2	Fluid properties and simulation parameters . . . . .	161
7.2.3	Grid independence study . . . . .	162
7.2.4	Validation of the numerical model . . . . .	163
7.3	Results and discussion . . . . .	164
7.3.1	Effect of Reynolds number . . . . .	164
7.3.2	Effect of degree of Subcooling . . . . .	171
7.4	Summary . . . . .	177
<b>8</b>	<b>Conclusions and Suggestions for Future Work</b>	<b>179</b>
8.1	Introduction . . . . .	179
8.2	Major conclusions . . . . .	180
8.3	Suggestions for future work . . . . .	182

## List of Figures

1.1	Nucleate Boiling (Alavi <i>et al.</i> , 2008). . . . .	1
1.2	Transition Boiling (Westwater, 1956). . . . .	2
1.3	Film Boiling (Jordan, 1969). . . . .	2
1.4	Condensation (Preston <i>et al.</i> , 2015). . . . .	3
1.5	Direct numerical simulation of film boiling over a flat plate (Juric and Tryggvason, 1998). . . . .	5
1.6	Volume of Fluid method. . . . .	6
1.7	Level Set method. . . . .	7
1.8	MOF reconstruction of linear interface (Dyadechko and Shashkov, 2008). $\omega$ is the reconstructed linear subcell whose centroid $\mathbf{x}_c(\omega)$ is closest to the true material centroid $\mathbf{x}^*$ . . . . .	8
2.1	Front tracking method: Transport equations are solved on a fixed Eulerian grid and the interface is tracked explicitly by marker points. (Tryggvason <i>et al.</i> , 2001) . . . . .	12
2.2	Geometric advection of VOF. . . . .	14
2.3	Comparison of the different interface reconstruction procedures (Dyadechko and Shashkov, 2005). . . . .	17
3.1	$L_1$ error versus $1/\text{CFL}$ for the translation test. . . . .	36
3.2	Normalised $L_1$ error versus $1/h$ for the translation test. . . . .	37
3.3	Comparison of the initial shape and the final shape obtained after one complete rotation of the slotted disk for different grids (colour: initial shape, colour:final shape). . . . .	38
3.4	Interface evolution of the circular fluid element in reversible vortex test for different grids. . . . .	41
3.5	Results of the rising bubble test case in comparison with the results of Hysing <i>et al.</i> (2009). (a) Rise velocity ( $v_c$ ), (b) Circularity ( $\psi$ ) and (c) Bubble centroid ( $y_c$ ). . . . .	45
3.6	Interface evolution for film boiling over a flat plate. . . . .	46
3.7	Temporal evolution of $Nu_{s,Avg}$ (shown in solid red colour) along with $Nu_{st,Avg}$ (shown in dashed blue colour) for natural convection film boiling over a flat plate at $\Delta T = 5K$ . . . . .	48

3.8	Natural convection film boiling over a cylinder at $\Delta T = 5K$ . . . . .	49
3.9	Natural convection film boiling over a cylinder at $\Delta T = 10K$ . . . . .	49
3.10	Temporal evolution of $Nu_{s,Avg}$ (shown in solid red colour) along with $Nu_{st,Avg}$ (shown in dashed blue colour) for natural convection film boiling over a cylinder at different wall superheats. . . . .	51
4.1	Schematic of flow film boiling over a system of two cylinders . . . . .	56
4.2	Representative mesh used for the computations. (a) Computation grid, (b) Closer view of two cylinders and (c) Closer view of the front cylinder. . . .	58
4.3	interface structure at an instant of $t = 0.5s$ obtained with different meshes	59
4.4	Vapour dynamics for different Reynolds numbers in the mixed regime at $Ja_v/Pr_v = 0.3$ and non-dimensional spacing of 4.0. (a) $Re_D = 50$ , (b) $Re_D = 100$ and (c) $Re_D = 150$ . . . . .	64
4.5	interface evolution for the case of $Re_D = 50$ , $Ja_v/Pr_v = 0.3$ and $\xi = 4.0$ . .	65
4.6	Steady interface evolution for the case of $Re_D = 100$ , $Ja_v/Pr_v = 0.3$ and $\xi = 4.0$ . . . . .	67
4.7	interface evolution for the case of $Re_D = 150$ , $Ja_v/Pr_v = 0.3$ and $\xi = 4.0$ .	67
4.8	Instantaneous space averaged Nusselt number values ( $\overline{Nu}_D$ ) for front (shown in red colour) and rear (shown in black colour) cylinders at different Reynolds number values for the case of $Ja_v/Pr_v = 0.3$ and $\xi = 4.0$ . $\overline{Nu}_D$ for (a) $Re_D = 50$ , (b) $Re_D = 100$ and (c) $Re_D = 150$ . Space-time averaged Nusselt number values are shown in (d). . . . .	69
4.9	interface evolution and instantaneous streamlines for $Re_D = 50$ , $Ja_v/Pr_v = 0.3$ and $\xi = 4.0$ . . . . .	71
4.10	interface and instantaneous streamlines for $Re_D = 50$ , $Ja_v/Pr_v = 0.6$ and $\xi = 4.0$ . . . . .	72
4.11	interface and instantaneous streamlines for $Re_D = 50$ , $Ja_v/Pr_v = 0.9$ and $\xi = 4.0$ . . . . .	72
4.12	Instantaneous space averaged Nusselt number values ( $\overline{Nu}_D$ ) for the front (shown in red colour) and the rear (shown in black colour) cylinders at different non-dimensional wall superheat values for the case of $Re_D = 50$ and $\xi = 4.0$ . $\overline{Nu}_D$ for (a) $Ja_v/Pr_v = 0.3$ , (b) $Ja_v/Pr_v = 0.6$ and (c) $Ja_v/Pr_v = 0.9$ . (d) Space-time averaged Nusselt number ( $\overline{Nu}_{D,t}$ ). . . . .	74
4.13	Interface evolution along with instantaneous streamlines for the case of $Re_D = 100$ and $\xi = 4.0$ at different non-dimensional wall superheats. (a) $Ja_v/Pr_v = 0.3$ , (b) $Ja_v/Pr_v = 0.6$ and (c) $Ja_v/Pr_v = 0.9$ . . . . .	76

4.14	Instantaneous space averaged Nusselt number values ( $\overline{Nu}_D$ ) for front (shown in red colour) and rear (shown in black colour) cylinders at different non-dimensional wall superheat values for the case of $Re_D = 100$ and $\xi = 4.0$ . $\overline{Nu}_D$ for (a) $Ja_v/Pr_v = 0.3$ , (b) $Ja_v/Pr_v = 0.6$ and (c) $Ja_v/Pr_v = 0.9$ . (d) Space-time averaged Nusselt numbers ( $\overline{Nu}_{D,t}$ ). . . . .	77
4.15	Interface evolution along with instantaneous streamlines for the case of $Re_D = 150$ and $\xi = 4.0$ at different non-dimensional wall superheats. (a) $Ja_v/Pr_v = 0.3$ , (b) $Ja_v/Pr_v = 0.6$ and (c) $Ja_v/Pr_v = 0.9$ . . . . .	79
4.16	Instantaneous space averaged Nusselt number values ( $\overline{Nu}_D$ ) for front (shown in red colour) and rear (shown in black colour) cylinders at different non-dimensional wall superheat values for the case of $Re_D = 150$ and $\xi = 4.0$ . $\overline{Nu}_D$ for (a) $Ja_v/Pr_v = 0.3$ , (b) $Ja_v/Pr_v = 0.6$ and (c) $Ja_v/Pr_v = 0.9$ . Space-time averaged Nusselt number ( $\overline{Nu}_{D,t}$ ) values are shown in (d). . . . .	80
4.17	Interface evolution at $Re_D = 50$ and $Ja_v/Pr_v = 0.3$ for different non-dimensional cylinder spacing values. (a) $\xi = 2.0$ , (b) $\xi = 4.0$ and (c) $\xi = 6.0$ . . . . .	81
4.18	One bubble ebullition cycle for $Re_D = 50$ , $Ja_v/Pr_v = 0.3$ and $\xi = 2.0$ . . . . .	83
4.19	One bubble ebullition cycle for $Re_D = 50$ , $Ja_v/Pr_v = 0.3$ and $\xi = 4.0$ . . . . .	83
4.20	One bubble ebullition cycle for $Re_D = 50$ , $Ja_v/Pr_v = 0.3$ and $\xi = 6.0$ . . . . .	83
4.21	Instantaneous space averaged Nusselt number values ( $\overline{Nu}_D$ ) for front (shown in red colour) and rear (shown in black colour) cylinders at different non-dimensional wall superheat values for the case of $Re_D = 50$ and $Ja_v/Pr_v = 0.3$ . $\overline{Nu}_D$ for (a) $\xi = 2.0$ , (b) $\xi = 4.0$ and (c) $\xi = 6.0$ . (d) Space-time averaged Nusselt number ( $\overline{Nu}_{D,t}$ ). . . . .	85
4.22	Space-time averaged Nusselt number ( $\overline{Nu}_{D,t}$ ) versus non-dimensional spacing between cylinders ( $\xi$ ) plots for front (shown in red) and rear (shown in black) cylinders at $Ja_v/Pr_v = 0.3$ for (a) $Re_D = 100$ and (b) $Re_D = 150$ . . . . .	87
5.1	Schematic of the present problem under study. . . . .	92
5.2	Typical mesh used in the simulations. (a) Computation mesh, (b) closer view of the two cylinders and (c) closer view of the upstream cylinder. . . . .	95
5.3	Interfaces obtained at time $t = 0.43$ s with different meshes. . . . .	96
5.4	$\overline{Nu}_{D,t}$ values obtained with the present solver and corresponding values of Singh and Premachandran (2019) for flow film boiling of saturated water at a pressure of 21.9 MPa for different Reynolds number and dimensionless wall superheat values. . . . .	97
5.5	Vorticity contours showing different modes of vortex shedding. (a) Mode-Ia: Single shear layer shedding, (b) Mode-Ib: Elongated single shear layer shedding, (c) Mode-II: Elongated shear layer with suppression of the shear layer shedding and (d) Mode-III: Separated shear layers shedding. . . . .	99

5.6	Zoomed view of Mode-III type of vortex shedding focusing on the shear layers near the cylinder walls. . . . .	101
5.7	Interface evolution for the case of $Ja_v/Pr_v = 0.3$ and $\xi = 4.0$ at (a) $Re_D = 50$ , (b) $Re_D = 100$ and (c) $Re_D = 150$ . . . . .	103
5.8	Instantaneous streamlines and interface morphology at $Re_D = 50$ for the case of $\xi = 4.0$ and $Ja_v/Pr_v = 0.3$ . . . . .	104
5.9	Instantaneous streamlines and interface morphology at $Re_D = 100$ for the case of $\xi = 4.0$ and $Ja_v/Pr_v = 0.3$ . . . . .	105
5.10	Instantaneous streamlines and interface morphology at $Re_D = 150$ for the case of $\xi = 4.0$ and $Ja_v/Pr_v = 0.3$ . . . . .	106
5.11	Time evolution of space averaged Nusselt number ( $\overline{Nu}_D$ ) values for the upstream (red colour) and downstream (black colour) cylinders for the case of $Ja_v/Pr_v = 0.3$ and $\xi = 4.0$ at (a) $Re_D = 50$ , (b) $Re_D = 100$ and (c) $Re_D = 150$ . (d) $\overline{Nu}_{D,t}$ value for each Reynolds number case. . . . .	109
5.12	Fast Fourier Transform of $\overline{Nu}_D$ signals of upstream (red colour) and downstream (black colour) cylinders for the case of $Ja_v/Pr_v = 0.3$ and $\xi = 4.0$ at (a) $Re_D = 50$ , (b) $Re_D = 100$ and (c) $Re_D = 150$ . . . . .	110
5.13	Instantaneous streamlines and interface morphology at $Ja_v/Pr_v = 0.3$ for the case of $Re_D = 150$ and $\xi = 6.0$ . . . . .	111
5.14	Instantaneous streamlines and interface morphology at $Ja_v/Pr_v = 0.6$ for the case of $Re_D = 150$ and $\xi = 6.0$ . . . . .	112
5.15	Instantaneous streamlines and interface morphology at $Ja_v/Pr_v = 0.9$ for the case of $Re_D = 150$ and $\xi = 6.0$ . . . . .	113
5.16	Contours of non-dimensional vorticity depicting the instability in the shear layer during the transition in the vortex shedding modes for the case of $Ja_v/Pr_v = 0.6$ , $Re_D = 150$ and $\xi = 6.0$ . . . . .	114
5.17	Contours of non-dimensional vorticity depicting the instability in the shear layer during transition in the vortex shedding modes for the case of $Ja_v/Pr_v = 0.9$ , $Re_D = 150$ and $\xi = 6.0$ . . . . .	115
5.18	Time evolution of $\overline{Nu}_D$ values for the upstream (red colour) and downstream (black colour) cylinders for the case of $Re_D = 150$ and $\xi = 6.0$ at (a) $Ja_v/Pr_v = 0.3$ , (b) $Ja_v/Pr_v = 0.6$ and (c) $Ja_v/Pr_v = 0.9$ . (d) $\overline{Nu}_{D,t}$ value for each dimensionless wall superheat case. . . . .	117
5.19	Instantaneous streamlines and interface morphology at $\xi = 2.0$ for the case of $Re_D = 100$ and $Ja_v/Pr_v = 0.6$ . . . . .	120
5.20	Instantaneous streamlines and interface morphology at $\xi = 4.0$ for the case of $Re_D = 100$ and $Ja_v/Pr_v = 0.6$ . . . . .	121
5.21	Instantaneous streamlines and interface morphology at $\xi = 6.0$ for the case of $Re_D = 100$ and $Ja_v/Pr_v = 0.6$ . . . . .	122

5.22	Shear layer instability and transition between Mode-Ib and Mode-III type of vortex shedding in the case of $\xi = 6.0$ for $Re_D = 100$ and $Ja_v/Pr_v = 0.6$ . . . . .	124
5.23	Time evolution of $\overline{Nu}_D$ values for the upstream (red colour) and downstream (black colour) cylinders for the case of $Re_D = 100$ and $Ja_v/Pr_v = 0.6$ at (a) $\xi = 2.0$ , (b) $\xi = 4.0$ and (c) $\xi = 6.0$ . (d) $\overline{Nu}_{D,t}$ values for each dimensionless spacing case. . . . .	126
6.1	Flux-based advection scheme of Dyadechko (2006) . . . . .	133
6.2	Volume conserved flux polygon construction. . . . .	139
6.3	Subdivided polygon. . . . .	140
6.4	Advection of first moment through face $ab$ . . . . .	141
6.5	Comparison of the interfaces at $t = T/2$ and $T$ for the translation test on a structured mesh. (a) Present MOF result and (b) MOF result of Dyadechko (2006). . . . .	146
6.6	Interface evolution of the circular fluid element in reversible vortex test for a structured mesh. . . . .	147
6.7	Interface evolution of the circular fluid element in reversible vortex test for an unstructured mesh. . . . .	147
6.8	Comparison of the initial and final interfaces for the reversible vortex test for a cell size of $1/128$ . (a) Present MOF result, (b) CLSVOF result of Kumar and Premachandran (2022), (c) MOF result of Mukundan <i>et al.</i> (2022) and (d) CLSVOF result of Mukundan <i>et al.</i> (2022). . . . .	148
6.9	Interface evolution for the Rayleigh-Taylor instability test case. (a) Present MOF method and (b) results of Zuzio and Estivalezes (2011) result. . . . .	151
6.10	Interface evolution for the rising bubble test. . . . .	153
6.11	Results of the rising bubble test case in comparison with the results of Hysing <i>et al.</i> (2009). (a) Rise velocity ( $v_c$ ), (b) Circularity ( $\psi$ ) and (c) Bubble centroid ( $y_c$ ). . . . .	154
6.12	Interface evolution for film boiling over a flat surface. . . . .	155
6.13	Temporal evolution of $Nu_{s,Avg}$ for film boiling over a flat surface. . . . .	157
7.1	Schematic of flow film boiling over a cylinder . . . . .	160
7.2	Typical mesh used in the simulations condensation over a cylinder. (a) Computation mesh, (b) closer view of the mesh near the cylinder. . . . .	162
7.3	Interface evolution for the case of $\Delta T = 10K$ at $Re_D = 10$ . . . . .	165
7.4	Interface evolution for the case of $\Delta T = 10K$ at $Re_D = 50$ . . . . .	166
7.5	Interface evolution for the case of $\Delta T = 10K$ at $Re_D = 100$ . . . . .	167

7.6	LIC along with the temperature contour for the case of $\Delta T = 10\text{K}$ and $Re_D = 10$ . . . . .	168
7.7	LIC along with the temperature contour for the case of $\Delta T = 10\text{K}$ at (a) $Re_D = 50$ and (b) $Re_D = 100$ . . . . .	169
7.8	Time evolution of space averaged Nusselt number ( $\overline{Nu}_D$ ) values for the case of $\Delta T = 10\text{K}$ at (a) $Re_D = 10$ , (b) $Re_D = 50$ and (c) $Re_D = 100$ . (d) $\overline{Nu}_{D,t}$ value for each Reynolds number case. . . . .	170
7.9	Interface evolution for the case of $Re_D = 100$ at $\Delta T = 2\text{K}$ . . . . .	171
7.10	Interface evolution for the case of $Re_D = 100$ at $\Delta T = 5\text{K}$ . . . . .	172
7.11	Interface evolution for the case of $Re_D = 100$ at $\Delta T = 15\text{K}$ . . . . .	173
7.12	LIC along with the temperature contour for the case of $Re_D = 100$ and $\Delta T = 2\text{K}$ . . . . .	174
7.13	LIC along with the temperature contour for the case of $Re_D = 100$ at (a) $\Delta T = 5\text{K}$ and (b) $\Delta T = 15\text{K}$ . . . . .	175
7.14	Time evolution of space averaged Nusselt number ( $\overline{Nu}_D$ ) values for the case of $Re_D = 100$ at (a) $\Delta T = 2\text{K}$ , (b) $\Delta T = 5\text{K}$ and (c) $\Delta T = 15\text{K}$ . (d) $\overline{Nu}_{D,t}$ value for each subcooling case. . . . .	176

## List of Tables

3.1	$L_2$ error norm for the slotted disk rotation test. . . . .	39
3.2	$L_1$ error norm for the reversible vortex test case . . . . .	40
3.3	Error estimates for the static bubble test . . . . .	43
3.4	Fluid properties of water at 21 900 kPa and 646.0 K ( $h_{lg} = 276\,400$ J/kg, $\sigma = 0.000\,07$ N/m, ). . . . .	46
3.5	Present $Nu_{st,Avg}$ values along with those available in the literature for film boiling over a flat surface. . . . .	48
3.6	Fluid properties of water at 21 900 kPa and 646.0 K ( $h_{lg} = 276\,400$ J/kg, $\sigma = 0.000\,07$ N/m, ). . . . .	50
3.7	Present $Nu_{st,Avg}$ values along with those available in the literature for film boiling over a cylinder. . . . .	52
4.1	Fluid properties of water at a pressure of 21.9 MPa and temperature 646 K ( $\sigma = 0.07$ mN/m, $h_{lg} = 276.4$ kJ/kg). . . . .	57
4.2	Space-time averaged Nusselt number values for each mesh . . . . .	59
4.3	Thermo-physical properties of Nitrogen at pressure of 1.836 MPa ( $\sigma = 1.5742$ mN/m, $h_{lv} = 120.241$ kJ/kg) . . . . .	60
4.4	Values of space-time averaged Nusselt number, $\overline{Nu}_{D,t}$ obtained in the present study with corresponding experimental values of Sakurai <i>et al.</i> (1990 <i>b</i> ) for saturated film boiling of nitrogen at a pressure of 1.836 MPa at different wall superheats . . . . .	60
4.5	Thermo-physical properties of water at near critical condition ( $p/p_c = 0.99$ ) ( $\sigma = 0.07$ mN/m, $h_{lv} = 276.4$ kJ/kg) . . . . .	61
4.6	Values of space-time averaged Nusselt number, $\overline{Nu}_{D,t}$ obtained in the present study with corresponding values available in the literature for water at critical condition ( $p/p_c = 0.99$ ) and various Reynolds numbers and non-dimensional wall superheats . . . . .	61
4.7	Comparison of space-time averaged Nusselt number ( $\overline{Nu}_{D,t}$ ) for natural convection film boiling over a cylinder . . . . .	62
5.1	Fluid properties of water at pressure of 21.9 MPa and temperature 646 K ( $\sigma = 0.07$ mN/m, $h_{lg} = 276.4$ kJ/kg). . . . .	93

5.2	Characteristics of different meshes used to obtain grid size independent solutions along with the $\overline{Nu}_{D,t}$ values of the two cylinders obtained for each mesh. . . . .	94
5.3	Fluid properties of Nitrogen at a pressure of 1.836 MPa ( $\sigma = 1.5742mN/m, h_{lg} = 120.241kJ/kg$ ). . . . .	96
6.1	For the reversible vortex test case, the $L_1$ error norm. . . . .	149
6.2	Error estimates for the static bubble test . . . . .	150
6.3	Fluid properties of water at 21 900 kPa and 646.0 K ( $h_{lg} = 276 400 J/kg, \sigma = 0.000 07 N/m$ ). . . . .	155
6.4	Present $Nu_{st,Avg}$ values along with those available in literature for film boiling over a flat surface. . . . .	157
7.1	Fluid properties of refrigerant R-123 at a pressure of 3.6 MPa and temperature 455.8 K ( $\sigma = 0.0307mN/m, h_{lg} = 25.4kJ/kg$ ). . . . .	161
7.2	Different meshes used to obtain grid size independent solutions along with the $\overline{Nu}_{D,t}$ values of the cylinder obtained for each mesh. . . . .	163
7.3	Nusselt number obtained with the present solver with corresponding correlation values of Nusselt (1916) and modified Nusselt correlation (Rohsenow, 1956) for film condensation of saturated refrigerant R-123 at a pressure of 3.6 MPa for different degrees of subcooling. . . . .	164

## NOMENCLATURE

$A$	heat transfer surface area, m <sup>2</sup>
$c_p$	specific heat capacity at constant pressure, J/Kg-K
$D$	diameter of cylinder, m
$F$	volume fraction
$F_{gen}$	volume fraction generation due to mass transfer s <sup>-1</sup>
$F_{st}$	Surface tension force, N/m <sup>3</sup>
$Fr$	Froude number
$g$	acceleration due to gravity, m/s <sup>2</sup>
$Gr$	Grashof number
$h$	grid size, m
$h_{lg}, h_{lv}$	latent heat of vapourisation, J/Kg
$Ja$	Jacob number
$\dot{m}$	mass flux, kg/s-m <sup>2</sup>
$\mathbf{n}$	unit normal to interface
$\mathcal{M}_0$	Zeroth moment of fluid, m <sup>3</sup>
$\mathcal{M}_1$	First moment of fluid, m <sup>4</sup>
$Nu$	Nusselt number
$\overline{Nu}_D$	Space averaged number
$\overline{Nu}_{D,t}$	Space-time averaged number
$p$	pressure, Pa
$Pr$	Prandtl number
$q''$	heat flux at interface, J/s-m <sup>2</sup>
$Re$	Reynolds number
$s$	Spacing between cylinders, m

$t$	time, s
$T$	Temperature, K
$\Delta T_{sub}$	degree of subcooling, K
$\Delta T_{sup}$	wall superheat, K
$U$	Velocity magnitude, m/s
$\mathbf{V}$	Velocity vector, m/s
$\mathbf{V}_{mt}$	Velocity vector at interface due to mass transfer, m/s
$V_c$	Volume of cell, m <sup>3</sup>
$\mathbf{x}_\Omega$	Material centroid

### Greek Symbols

$\phi$	Level set, m
$\tau$	non-dimensional time
$\omega$	vorticity, 1/s
$\Omega$	non-dimensional vorticity
$\lambda_0$	characteristic length scale, m
$\xi$	non-dimensional spacing between cylinders
$\rho$	density, kg/m <sup>3</sup>
$\mu$	viscosity, Pa.s
$\kappa$	conductivity, W/m-K
$\sigma$	coefficient of surface tension, N/m

### Subscripts

$cell$	cell
$\infty$	free stream condition
$v, g$	vapour
$l$	liquid
$sat$	saturation

### Abbreviations

**ACLSVOF** Adaptive Coupled Level Set and Volume Of Fluid

**AMR-MOF** Adaptive Mesh Refinement strategy based on Moment Of Fluid

<b>CFL</b>	Courant-Friedrichs-Lewy conditions
<b>CLSMOF</b>	Coupled Level Set Moment Of Fluid
<b>CLSVOF</b>	Coupled Level Set and Volume Of Fluid
<b>CSF</b>	Continuum Surface Force
<b>EI-LE</b>	Eulerian-Implicit and Lagrangian-Explicit
<b>ELVIRA</b>	Efficient Least squares Volume of fluid Interface Reconstuction Algorithm
<b>EMFPA</b>	Edge Matched Flux Polgygon Advection
<b>FFT</b>	Fast Fourier Transform
<b>FMFPA</b>	Face Matched Flux Polgygon Advection
<b>HF</b>	Height Function
<b>LBM</b>	Lattice Boltzmann Method
<b>LS</b>	Level Set
<b>LVIRA</b>	Least squares Volume of fluid Interface Reconstuction Algorithm
<b>MOF</b>	Moment Of Fluid
<b>PLIC</b>	Piecewise Linear Interface Calculation
<b>PROST</b>	Parabolic Reconstruction of Surface Tension
<b>SIMPLE</b>	Semi-Implicit Method for Pressure Linked Equations
<b>SIR</b>	Spline Interface Reconstruction
<b>SL-VOF</b>	Segment-Lagrangian Volume Of Fluid
<b>TVD</b>	Total Variation Dimnishing
<b>ULA</b>	Unsplit Lagrangian Advection
<b>VOF</b>	Volume Of Fluid
<b>VOF-CISIT</b>	Volume Of Fluid based Conservative Interpolation Scheme for Interface Tracking
<b>VOSET</b>	coupled Volume Of fluid and level SET